START PAGE

Chapter 15

CONTROL OF ELECTRIC GENERATORS

15.1. INTRODUCTION

Practically all electric energy is produced through electric generators driven by prime-movers. The solar power panels are the notable exception.

The prime-movers extract their mechanical energy from the water or wind energy, from steam (by burning oil or coal nuclear or fuel) or gas – burning thermal energy, gasoline or Diesel fuel in internal combustion engines (ICE).

The prime-movers are basically wind, hydro, steam turbines or ICEs.

The standard is that electric energy is produced in power plants with the prime-movers (turbines) operated at controlled, almost constant, speed, through a speed governor that acts on the fuel input rate of the prime-movers.

Synchronous generators (up to 1400 MVA/unit) are used in standard power systems. They provide controlled constant voltage (through their DC rotor excitation current control) and constant frequency ($f_n = n_n p$) through prime mover speed control.

Regional, national and continental electric power systems have been built by adding synchronous generators in parallel.

The rather weak coupling between the frequency (active power) and voltage (reactive power) control in synchronous generators works well in stiff power systems with sizeable spinning power reserves.

The recent opening of electrical energy markets leads to the separation of electric energy production, transmission and distribution to customers. Also, decentralization in energy production is accentuating and results in more distributed electric power systems.

The tendency to produce the daily peaks of electric energy closest to their consumption has led to smaller generator units, with variable output.

The tighter environmental requirements have prompted more renewable energy conversion systems. Wind (up to 4 MW/unit) and hydro energy (up to 770 MW/unit) are typical renewable energy sources with a softer effect on the environment.

In distributed electric power systems, the coproduction of heat and electricity is proposed through super high speed gas turbine – electric generators up to 3 MVA/unit at 15000 rpm or 100 KVA/unit at 70000 rpm. Small companies, villages or town sections may profit from such highly efficient decentralized energy production solutions.

Autonomous generators sets, driven mainly by gas turbines or ICE, even by small hydro or wind turbines, are also used for emergency (or standby)

power in Telecom, hospitals, banks, etc with power/unit up to a few hundred KW.

Finally, more and more electric energy on board vehicles is needed for better comfort, better gas-mileage in standard ICE vehicles, but also for the newly developed hybrid electric vehicles (HEV). Electric machines on HEV for powers up to 100 kW and more should work both as motors, for vehicle propulsion assistance, and as electric generators for battery recharging and electrical vehicle braking.

Large and medium power synchronous generators in power systems are controlled in terms of voltage (reactive power), while the frequency (speed) or active power is controlled through the mechanical prime-mover's speed governor.

In the distributed power systems of the future, fast active power and voltage control may be harnessed better when variable speed is allowed for.

Variable speed electric generators imply power electronics converter interfaces to produce constant voltage and frequency output.

Wind and small hydro turbine electric generators are typical for almost mandatory variable speed control.

So full rating (100%) power electronic converters with electrically, excited, or PM, synchronous generators, or cage-rotor induction generators up to 4-10MW are to be expected.

Partial rating (20-30%) power electronic converters connected to the wound rotor of induction generators have already been introduced for limited (±20-5%) speed control range up to 400 MVA in pump-storage hydropower plants.

Switched reluctance generators with full rating power electronics control have been proposed for aircraft (up to 250KW) or for HEVs (up to 100 KW).

Also, full rating (100%) power electronics control PM brushless generators/motors are introduced as starter-alternators up to 100 KW and more, on board hybrid (or electric) vehicles.

In what follows we will concentrate on a few essential control aspects of electric generators, recommending the interested reader to go to Ref. 1 and then take it from there.

The main issues treated here are:

- Rather constant frequency (active power) and voltage (reactive power) control of synchronous generators connected to electric power systems.
- Limited variable speed wound-rotor induction generator control.
- Full power electronics control of variable speed PM synchronous generators.
- Full power electronics control of variable speed cage-rotor induction generators.
- The control of claw-pole rotor alternators on automobiles.
- IPM synchronous starter-alternator control on HEV.
- Switched reluctance generator output control at variable speed.

15.2. CONTROL OF SYNCHRONOUS GENERATORS IN POWER SYSTEMS

AC power systems operate satisfactorily when their frequency and voltage remain nearly constant and thus vary in a limited and controllable mover, when active and reactive power loads they serve are modified.

Active power flow is controlled by modifying the prime mover fuel flow rate to control the speed of the generator with a few percent variation range.

On the other hand, reactive power flow is related to generator terminal voltage control, within a few percent change range, by varying the DC field rotor winding current.

When too large an electric power load occurs, the speed may collapse. Similarly, too large a reactive power load leads to voltage collapse.

When a synchronous generator (SG) acts alone on its loads such as in generator sets or it is the largest by far in the respective power system, the former is controlled for constant (isochronous) speed.

In contrast, when an SG operates in a large power system, the load power is shared by many SGs. In this case it is mandatory to control the generator with a speed droop.

A voltage droop is required for voltage control, or to provide for reactive power load sharing between SGs.

Automatic generation control (AGC) divides the electric power generation between SGs, while the automatic reactive power control (AQC) distributes the reactive power contribution between same SGs.

As there is some coupling between P (active power) and Q (reactive power) controls, especially for weak power systems, power system stabilizers (PSS) are added for decoupling.

All these principles are visible in the general SG control system in Figure 15.1.

The speed governor and its controller and the frequency (speed)/power droop curve serve to control the speed to produce the required active power P^*.

The speed droop curve may be raised or lowered to decrease or increase the power share of the respective generator.

On the generator side, the voltage controller and limiters act on the voltage error $V_c^*-V_c$, corroborated with the PSS output. A voltage load compensator is added. It is beyond our scope here to explain the whole, multilevel, control system of an SG into a large power system ([1], Chapter 2).

We will concentrate a little only on SG exciters and on the automatic voltage regulator (AVR).

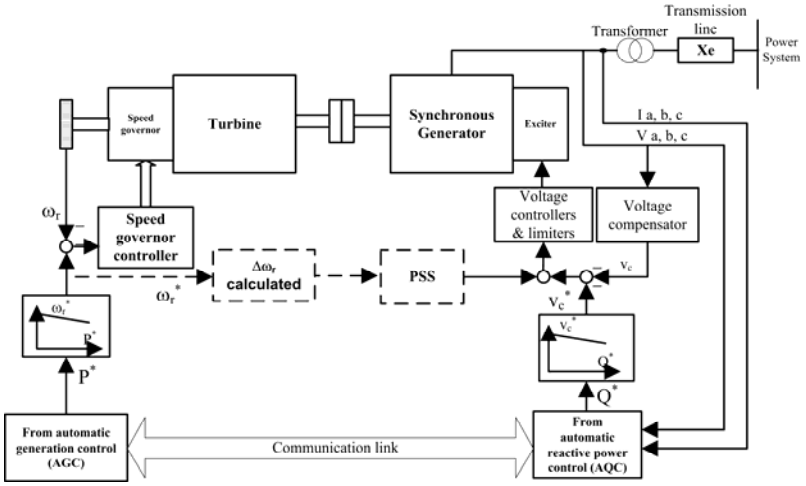

Figure 15.1. General SG control system

15.2.1. Exciters for SG

The exciter is an electric power source that is capable of supplying in a controllable manner the field winding of the SG such that the SG terminal voltage is satisfactorily controlled under designed active and reactive power load variation range.

There are two main types of exciters in fabrication today:

- AC brushless exciters
- static exciters

15.2.2. The AC brushless exciter

The standard AC brushless exciter (Figure 15.2) is made of an inside-out synchronous machine whose stator holds a DC fed field winding while its rotor contains the three phase (armature) winding and a diode rectifier which supplies directly the SG field winding. The stator-placed exciter DC field winding current is controlled through a small power static power converter, to provide controlled voltage at SG terminals.

It is evident that the time constant and transfer functions of both, SG and the AC brushless exciter (basically an inverted, small, 3%, rating SG), stand between the command voltage V_{con} at the output of the voltage regulator and the regulated terminal voltage of SG.

There is no easy way to measure any variable such as the SG field current or voltage and thus a very robust AVR is needed.

The time allowed for the field winding voltage V_f to rise from 0 to 95 % rated value is limited by standards to a few tens of milliseconds. On the other hand, forcing the voltage V_f to (1.5 - 3) times rated value V_{fn} is needed to produce acceptably fast terminal voltage response to perturbations.

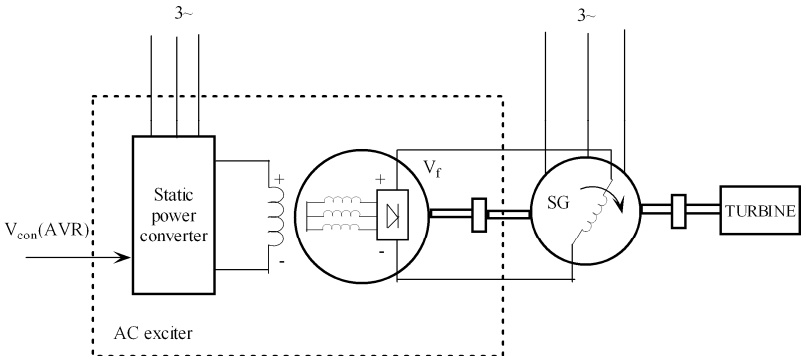

Figure 15.2. The AC brushless exciter

The AC brushless exciter has the inherent advantage that it is rather immune to SG faults, when the SG terminal voltage decreases notably, if the small power static converter (Figure 15.2) has a back-up source during SG faults or is fed from a rechargeable battery.

An approximate model of the AC exciter (alternator without a rotor cage) is shown in Figure 15.3.

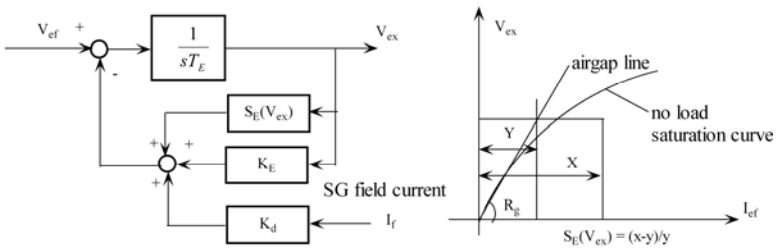

Figure 15.3. AC exciter alternator structural diagram for control

The load of the AC exciter alternator comes into play only through the SG field current I_f produced armature reaction in the a.c exciter. As the diode rectifier provides for almost unity power factor, I_f influence on V_{ex} regulation is rather straightforward (Figure 15.3).

S_E (V_{ex}) introduces the influence of the magnetic saturation in the AC exciter on the V_{ex} limitation. T_E is the AC exciter alternator excitation time constant.

The diode rectifier (Figure 15.4) introduces an additional voltage regulation and its model is needed also.

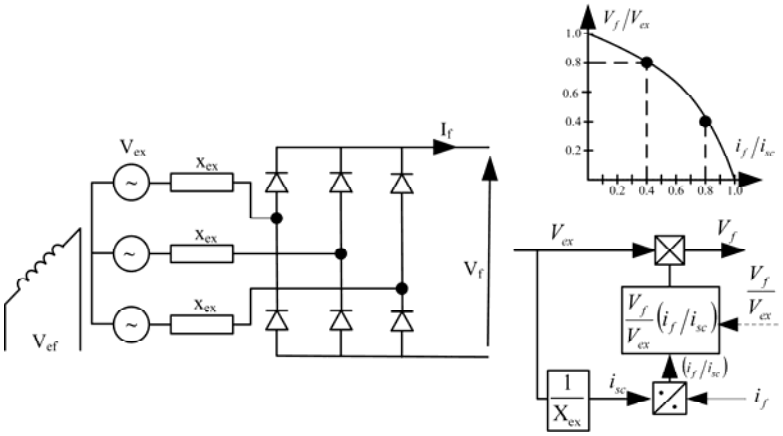

Figure 15.4. AC exciter alternator + diode rectifier

The V_f (I_f) output characteristic is rather nonlinear and depends heavily on diode commutation overlapping.

The AC exciter reactance (X_{ex}) plays a major role in the diode commutation process.

Three main operation modes may be identified:

Stage 1: two diodes conducting (low load):

$$\frac{V_f}{V_{ex}} \approx 1 - \frac{1}{\sqrt{3}} \frac{I_f}{I_{sc}} \quad \text{for} \quad \frac{I_f}{I_{sc}} < \left(1 - \frac{1}{\sqrt{3}}\right) \tag{15.1}$$

with

$$I_{sc} = \frac{V_{ex}\sqrt{2}}{X_{ex}} \tag{15.2}$$

Stage 2: each diode conducts only when the other one on the same leg ended conduction (medium load):

$$\frac{V_f}{V_{ex}} = \sqrt{\frac{3}{4} - \left(\frac{I_f}{I_{sc}}\right)^2} \quad \text{for} \quad \left(1 - \frac{1}{\sqrt{3}}\right) \le \frac{I_f}{I_{sc}} \le \frac{3}{4} \tag{15.3}$$

Stage 3: four diodes are conducting at any time:

$$\frac{V_f}{V_{ex}} = \sqrt{3}\left(1 - \frac{I_f}{I_{sc}}\right) \quad \text{for} \quad \frac{3}{4} \le \frac{I_f}{I_{sc}} \le 1 \tag{15.4}$$

Figure 15.4 illustrates eqns (15.1) – (15.4) and introduces the nonlinear structural diagram that represents the diode rectifier.

15.2.3. The static exciter

The standard static exciter for SGs is the fully controlled phase rectifier (Chapter 5) — Figure 15.5 where V_{ex}, X_{ex} represent the voltage and internal (transient) reactance of the power source (a transformer in general) that supplies the static exciter. The static exciter is placed on ground and thus it transmits the power to the SG field winding through brushes and copper slip rings.

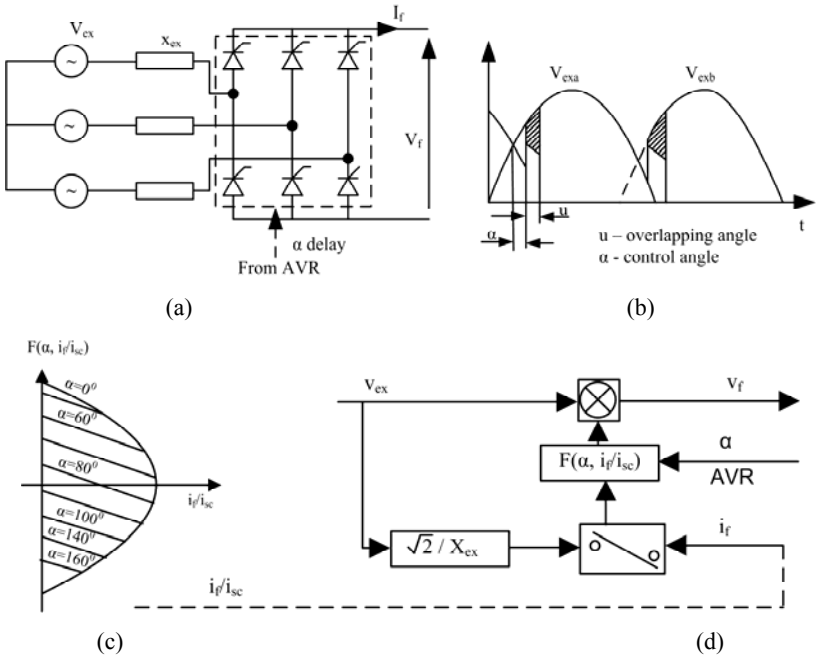

Figure 15.5. a.) The controlled rectifier as static exciter; b.)its output voltage waveform, c.) voltage/current curve, d.) nonlinear structural diagram

As shown in Chapter 5, the controlled rectifier output voltage V_f is:

$$V_f' = \frac{3\sqrt{2}V_{ex}\sqrt{3}\cos\alpha}{\pi} - \frac{3}{\pi}X_{ex}I_f;\ \ I_{sc} = \frac{V_{ex}\sqrt{2}}{X_{ex}} \tag{15.5}$$

Consequently:

$$\frac{V_f}{V_{ex}} = \cos\alpha - \frac{1}{\sqrt{3}}\frac{I_f}{I_{sc}};\ \ V_f = \frac{V_f'\pi}{3\sqrt{6}} \tag{15.6}$$

For $\alpha = 0$ – zero phase delay angle – (15.6) degenerates into (15.1): the diode rectifier.

With the exciter main parts already modeled here, only the automated voltage regulator (AVR) is still needed to complete the system.

Apart from standardized excitation — AVR systems such as IEEE 1992 AC1A (with AC brushless exciter) and IEEE 1992 ST1A (with static exciter) which are basically analog systems — let us consider here a digital PID AVR system.

15.2.4. A digital PID AVR system

The AC exciter is simplified (armature reaction is neglected) and the diode rectifier model is a gain, as in Figure 15.6. A proportional — derivative — integral (PID) voltage regulator is used.

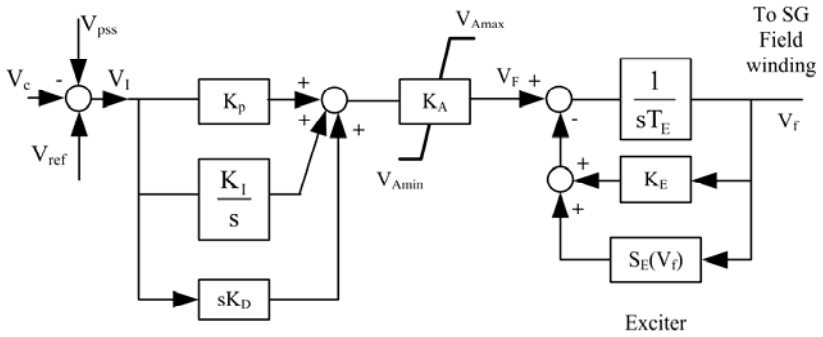

Figure 15.6. PID voltage regulator for SG

With a sampling frequency more than 20 times the damped frequency of the close loop system we may design the PID controller as if it were continuous, with:

$$G_c(s) = K_P + \frac{K_I}{s} + sK_D \tag{15.7}$$

with K_P – proportional gain, K_I integral gain, K_D – derivative gain.

As the exciter was considered here as a first order model (only one time constant, T_E), the SG may be modeled also as a first order system with the excitation time constant T'_{d0}, at constant speed and for small deviation transients.

Consequently, the AC exciter plus the SG exhibits a simplified second order transfer function G(s):

$$G(s) = \frac{l_{dm} / r_f (S_E + K_E)}{(1 + sT'_{d0}) \cdot (1 + sT_e)}; \quad T_e = \frac{T_E}{S_E + K_E}; \quad T'_{d0} = \frac{l_{dm} + l_{fl}}{\omega_b \cdot r_f} \tag{15.8}$$

Where l_{dm} is the SG magnetization inductance in P.U. and r_f is the SG field winding resistance in P.U.; l_{fl} is the SG field winding leakage inductance in P.U.; ω_b – the base (rated) angular frequency of the SG.

The closed loop system, which includes the PID controller, has the known characteristic equation:

$$G(s)\cdot G_c(s)+1=0 \tag{15.9}$$

Let us consider $l_{dm}/(r_f(S_E+K_E))=1$ for simplicity.

Making use now of (15.7) and (15.8) in (15.9) we obtain:

$$K_D^2 s^2 + K_P s + K_I = -s(1+sT'_{d0})(1+sT_e) \tag{15.10}$$

As it would be desirable to deal with a second order system, we select from the start a negative pole s_3=c in the left half-plane. The other two poles are chosen as complex and conjugate: $s_{1,2} = a \pm jb$.

The peak overshoot and settling time, or other method of pole placement, may be used to find the two remaining unknowns $s_{1,2}$ in (15.10) and thus to find the controller gains K_P, K_I, K_D.

The controller gains give rise to two zeros that might affect the transients unfavorably and thus, by trial and error, the final values of K_P, K_I, K_D are settled.

As an example, for T'_{d0}=1.5 s, T_e = 0.3 s, f_1 = 60 Hz, settling time = 1.5 s, peak overshoot = 10 %,a satisfactory analog PID controller gain set would be: K_P = 39.3, K_I = 76.5, K_D = 5.4 [3].

The conversion into discrete form may use the trapezoidal integration method:

$$s \to \frac{1-z^{-1}}{T};\ \frac{1}{s} \to \frac{T}{2}\frac{1+z^{-1}}{1-z^{-1}} \tag{15.11}$$

z^{-1} is the unit delay.

The PID controller discrete transfer function $G_c(z)$ is thus:

$$G_c(z)=\left[K_{PD}+\frac{K_{ID}}{1-z^{-1}}+K_{DD}(1-z^{-1})\right]\cdot K_{AA}=\frac{\Delta V_f(z)}{\Delta V_I(z)} \tag{15.12}$$

with $K_{PD}=K_P - K_I(T/2)$, $K_{ID}=K_IT$, $K_{DD}=K_D/T$.

The K_{AA} gain was added in (15.12).

Making use of the property: $z^{-1}X(k) = X(k-1)$ leads to the discrete form of the PID voltage controller output $\Delta F(k)$:

$$\begin{aligned}\Delta F(k) = \Delta F(k-1) + (K_{PD}+K_{ID}+K_{DD})\Delta V_I(k) - \\ -(K_{PD}+2K_{DD})\Delta V_I(k-1)+K_{DD}\Delta V_I(k-2)\end{aligned} \tag{15.13}$$

with ΔV_I as the SG voltage error variation (Figure 15.7).

For a 75KVA, 208 V, 0.8 PF (lagging) SG with T=12.5 ms, K_{PD}=777, K_{ID}=19, K_{DD}=8640, K_{AA}=7.00, a 50 KVAR reactive load application and

rejection response is shown in (Figure 15.7a). A step reference voltage response (up and down) is shown in Figure 15.7b.

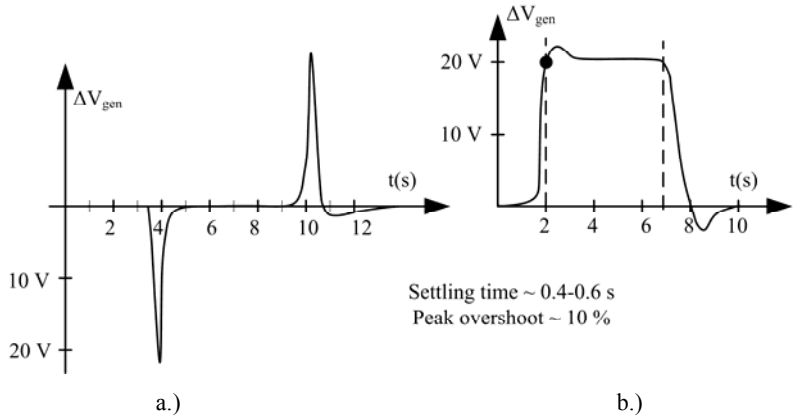

Figure 15.7. SG voltage response with PID AVR

Stable voltage response under severe reactive power surge is evident.

Note: The PID voltage regulator is a mere example of AVR and many other more robust configurations have been introduced. Among them the ones based on sliding mode and fuzzy logic stand out as apparently more practical.

15.3. CONTROL OF WOUND-ROTOR INDUCTION GENERATORS (WRIGs) WITH LIMITED SPEED RANGE

Wound-rotor induction motors have been treated in Chapter 14 for large power drive applications with limited speed control range.

The stator and rotor active power balance for steady state still holds (from Chapter 14):

$$P_s \approx -P_{Cos} + P_{elm};\ P_{elm} = \frac{T_e \omega_1}{p} \tag{15.14}$$

$$P_r \approx -p_{Cor} - SP_{elm};\ S = \frac{\omega_1 - \omega_r}{\omega_r} \tag{15.15}$$

P_{Cos} and P_{Cor} are the stator and rotor winding losses.

P_s, P_r positive means generated (delivered) electric powers; S is slip and is positive in sub-synchronous ($\omega_r < \omega_1$)and negative in super-synchronous ($\omega_r > \omega_1$) operation.

P_{elm} is the electromagnetic power, which again is positive for the generator operation mode. The torque T_e is considered positive for the generator mode ($\omega_1 = 2\pi f_1$, f_1 – stator frequency, p - pole pairs).

For generator mode in sub-synchronous operation, $P_s > 0, P_r < 0$, while for super - synchronous operation, $P_s > 0, P_r > 0$ (Figure 15.8).

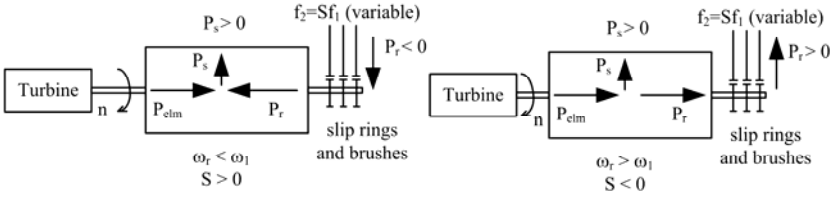

Figure 15.8. WRIG power balance: a.) sub-synchronous generator mode, b.) super-synchronous generator mode

The core and and mechanical losses have been neglected here, for more clarity.

It should be noted that the stator power P_s comes at frequency f_1 and the rotor electric power P_r at frequency $f_2 = Sf_1$ with $|f_2| < 0.2f_1$, in general.

Also f_1 = constant and f_2 is variable with speed:

$$f_1 = f_2 + np; \;\; n - \text{speed} \;\; (\text{rps}) \tag{15.16}$$

For super-synchronous operation ($n > f_1/p$), $f_2 < 0$, which means that the sequence of rotor phases (supplied through a static power converter) is changed form abc to acb.

For super-synchronous operation, say at $S_{max} = -0.25$, with copper losses neglected, $P_r > 0$ and thus the total power of WRIG is:

$$P_{max} = P_{elm} + |S_{max}| \cdot P_{elm} \tag{15.17}$$

The machine is electromagnetically designed for P_{elm}, at synchronous speed $n_1=f_1/p$ but, because it runs at larger speed $n_{max} = n(1+|S_{max}|)$, it produces additional electric power P_r through the rotor $P_r=|S_{max}| P_{elm}$. This is considered a notable cost advantage of WRIG.

The reactive power flow in WRIGs is not dependent on slip S sign, as expected, and we may magnetize the machine from the rotor side (through the static power converter) or from the stator. In addition, it may be feasible to work with reactive power delivery through the stator or the rotor — if the rotor-side converter is capable to provide it. Fortunately the ratio of the rotor reactive power Q_r (at f_2), necessary to produce a reactive power Q_s (at f_1), is:

$$\frac{Q_r}{Q_s} = \frac{f_2}{f_1} = S \tag{15.18}$$

This is so because the magnetic energy, which is conserved, does not depend on frequency.

To limit the costs of the rotor side converter, WRIGs in general are operated at best at unity power factor in the stator. In this case the current

oversizing of the rotor static power converter over $|S_{max}|$ P_{elm} is not larger than 10 – 15 %, to provide for the reactive power required to magnetize the machine.

Typical static power converters used for the scope are:

- Back to back voltage source two (or multi) level PWM converters;
- Cycloconverters;
- Matrix converters;

They all provide 4 quadrant operation (Figure 15.9) but only back to back PWM converters and matrix converters have enough secondary frequency range to provide the starting of the machine as a motor (in pump storage applications) from the rotor side with short-circuited stator.

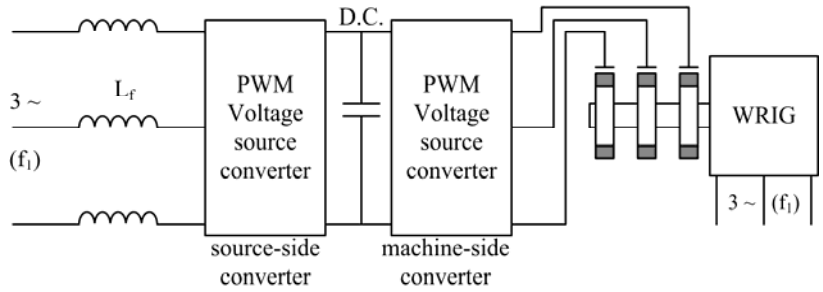

Figure 15.9. Bidirectional back to back PWM converter for the rotor of WRIGs

The two converters in Figure 15.9 are practically identical and constitute the typical two (or multi) level voltage source PWM converter used for AC drives.

There is a filter L_f at the source side but the voltage-matching transformer to the AC source is missing. It is feasible to leave it out if we design the WRIG such that at maximum slip ($|S_{max}|$) the required rotor voltage V_{rmax} is equal to the constant stator voltage V_s:

$$V_{r\,max} \approx V_s \tag{15.19}$$

E_s and E_r are the stator and rotor e.m.f.s:

$$S_{max} E_s \frac{W_r K_{Wr}}{W_s K_{Ws}} = E_{r\,max} = V_{r\,max} \tag{15.20}$$

W_s, W_r are the numbers of turns per current path in the stator and, respectively, in the rotor, while K_{Ws}, K_{Wr} are the corresponding winding factors. For example, with $|S_{max}|$=0.25 and identical winding factors K_{Ws}=K_{Wr} W_r/W_s=4/1. This situation leads to a corresponding reduction of rotor rated current I_r: $I_r/I_s \cong 1/4$, as expected.

15.3.1. The space phasor model of WRIG

WRIG is a typical IM and thus the space phasor model developed in Chapter 8 stands here valid:

$$\bar{I}_s R_s + \bar{V}_s = -\frac{d\bar{\lambda}_s}{dt} - j\omega_b \bar{\lambda}_s;\ \ \bar{\lambda}_s = L_{sl}\bar{I}_s + L_m \bar{I}_m;\ \ \bar{I}_m = \bar{I}_s + \bar{I}_r$$

$$\bar{I}_r R_r + \bar{V}_r = -\frac{d\bar{\lambda}_r}{dt} - j(\omega_b - \omega_r)\bar{\lambda}_r;\ \ \bar{\lambda}_r = L_{rl}\bar{I}_r + L_m \bar{I}_m \tag{15.21}$$

The electromagnetic torque T_e ($T_e > 0$ for generating) is:

$$T_e = \frac{3}{2} p I_{mag}[\bar{\lambda}_s \bar{I}_s^*] = \frac{3}{2} p\left(\lambda_d I_q - \lambda_q I_d\right) \tag{15.22}$$

With d/dt=s, eqns (15.21) become:

$$\left(R_s + (s + j\omega_b)L_{sl}\right)\cdot \bar{I}_s + \bar{V}_s = -L_{mt} s(\bar{I}_s + \bar{I}_r) - j\omega_b L_m(\bar{I}_s + \bar{I}_r)$$

$$\left(R_r + (s + j(\omega_b - \omega_r))L_{rl}\right)\cdot \bar{I}_r + \bar{V}_r = -L_{mt} s(\bar{I}_s + \bar{I}_r) - j(\omega_b - \omega_r)L_m(\bar{I}_s + \bar{I}_r) \tag{15.23}$$

These equations lead to the equivalent circuit of Figure 15.10.

L_{mt} is the transient magnetization inductance while L_m is the steady state one, both depend on magnetization current I_m, due to magnetic saturation.

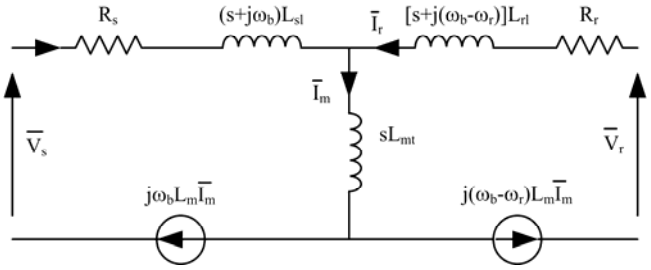

Figure 15.10. The space phasor equivalent circuit of WRIG

The speed of the reference system ω_b is free to choose but stator coordinates ($\omega_b = 0$), rotor coordinates ($\omega_b = \omega_r$) and synchronous coordinates ($\omega_s = \omega_1$) are favored, depending on the application.

For steady state $s \rightarrow j(\omega_1 - \omega_b)$ with ω_1 the frequency of actual stator variables (currents and voltages).

We may add two equations for the stator and rotor homopolar components, which are however independent of the space phasor components (Chapter 8):

$$I_{s0}R_s + V_{s0} \approx -L_{sl}\frac{dI_{s0}}{dt}$$
$$I_{r0}R_r + V_{r0} \approx -L_{rl}\frac{dI_{r0}}{dt} \qquad (15.24)$$

Note: In all equations above the rotor variables are reduced to the stator ones.

For steady state, the stator and rotor voltages in their phase coordinates, when symmetric, are:

$$V_{abc}(t) = V_s\sqrt{2}\cos(\omega_1 t - (i-1)\frac{2\pi}{3})$$
$$V_{ar\,br\,cr}(t) = V_r\sqrt{2}\cos((\omega_1 - \omega_r)t + \gamma_v - (i-1)\frac{2\pi}{3}) \qquad (15.25)$$

Also for steady state a simplified vector diagram is obtained by using eqn (15.23) with $s \rightarrow j(\omega_1-\omega_b)$.

In Figure 15.11 such a vector diagram is presented for unity power factor in the stator and sub-synchronous operation.

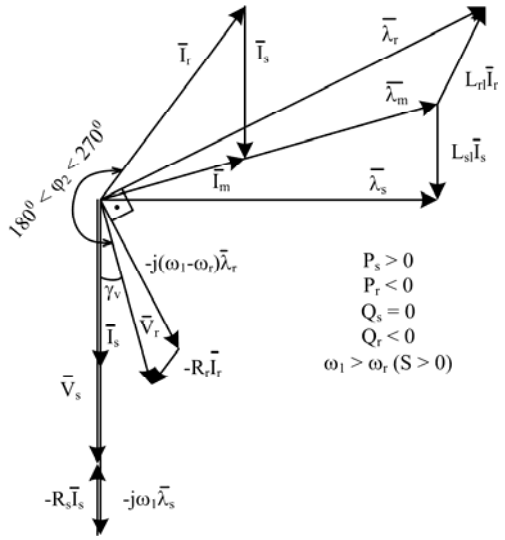

Figure 15.11. WRIG steady state vector diagram for sub-synchronous operation ($(\omega_1-\omega_b) > 0$) at unity stator power factor

A few remarks are in order:

- As the stator power factor is unity, the machine magnetization comes from the rotor and thus the rotor flux amplitude λ_r is larger than the stator flux amplitude λ_s.

- Also, the rotor power factor angle φ_2 is between 180° and 270° to provide for negative (drained) active and reactive rotor electric power.
- At zero slip (conventional synchronous speed, $\omega_1=\omega_r$) the vector diagram still holds but then $\overline{V}_r = \bar{I}_r R_r$ and the rotor flux λ_r loses its paramount role in explaining the machine behavior.

As the stator flux voltage and frequency (or stator flux) are kept rather constant, the reference system may be tied to stator voltage $\overline{V}_s$ or stator flux $\overline{\lambda}_s$, for vector control.

15.3.2. Vector control principles

Let us align the reference system to stator flux $\overline{\lambda}_s$:

$$\overline{\lambda}_s = \lambda_s = \lambda_d;\ \lambda_q = 0;\ \frac{d\lambda_q}{dt} = 0 \tag{15.26}$$

In dq coordinates, the stator equation in (15.21), with λ_s ~ constant and R_s ~0, becomes:

$$\begin{aligned} V_d &= 0;\ \lambda_q = L_s I_q + L_m I_{qr} = 0 \\ V_q &= -\omega_r \lambda_d;\ \lambda_d = L_s I_d + L_m I_{dr} \end{aligned} \tag{15.27}$$

Consequently, the stator active and reactive powers P_s, Q_s are:

$$\begin{aligned} P_s &= \frac{3}{2}(V_d I_d + V_q I_q) = \frac{3}{2} V_q I_q \approx \frac{3}{2}\omega_1 \lambda_d \frac{L_m I_{qr}}{L_s} \\ Q_s &= \frac{3}{2}(V_d I_q - V_q I_d) = \frac{3}{2}\omega_1 \lambda_d I_d = \frac{3}{2}\omega_1 \frac{\lambda_d}{L_s}(\lambda_d - L_m I_{dr}) \end{aligned} \tag{15.28}$$

If is now evident that, with constant stator flux amplitude (λ_d), the stator active power, P_s, may be controlled by I_{qr} (rotor q axis) current control, while stator reactive power, Q_s, control is performed through I_{dr} (rotor d axis) current control. This is in fact the principle of current vector control.

The rotor voltage equations, for steady state, in these conditions are simply:

$$V_{dr} = -R_r I_{dr} + L_{sc} S \omega_1 I_{qr} \tag{15.29}$$

$$V_{qr} = -R_r I_{qr} - S\omega_1 \left(\frac{L_m}{L_r} \lambda_d + L_{sc} I_{dr} \right) \tag{15.30}$$

Now eqns (15.29) - (15.30) pave the way for combined voltage / current vector control as they represent the voltage decoupling conditions.

15.3.3. Vector control of the machine side converter

Combined voltage/current vector control is straightforward using (15.28) - (15.30). Such a scheme is illustrated in Figure 15.12 where P_s and Q_s power controllers are added, and θ_s is the stator flux position angle with respects to phase a in the stator and θ_{er} is the rotor phase a_r axis position with respect to stator phase a, in electrical degrees.

Dual Park transformation is required first to bring the rotor currents into stator flux coordinates and then, once again, to "translate" the rotor voltages V_{dr}, V_{qr} into rotor coordinates.

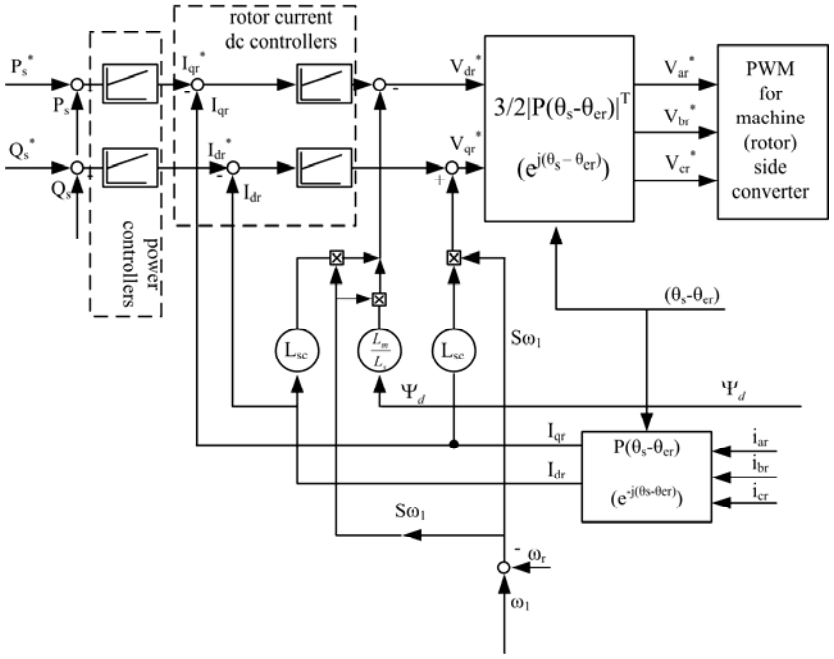

Figure 15.12. P_s, Q_s vector control of WRIG side converter

It is evident the stator voltages, stator currents and rotor currents have to be measured. The stator flux estimator is straightforward:

$$\bar{\lambda}_s = \bar{\lambda}_{s0} - \int (V_s + R_s I_s)\,dt \tag{15.31}$$

The offset in the integrator has to be taken care of. A first order delay replacement of the integrator might do it. This way the stator flux amplitude $\lambda_s=\lambda_d$ and angle θ_s are obtained.

The rotor position θ_{er} has to be either measured by a robust and precise encoder or may be estimated to provide for motion-sensorless control.

15.3.4. Rotor position estimation

For rotor position (θ_{er}) estimation we first have to investigate the angle relationships between rotor axis angle $\theta_{er,}$ stator flux angle θ_s and the rotor current vector (Figure 15.13).

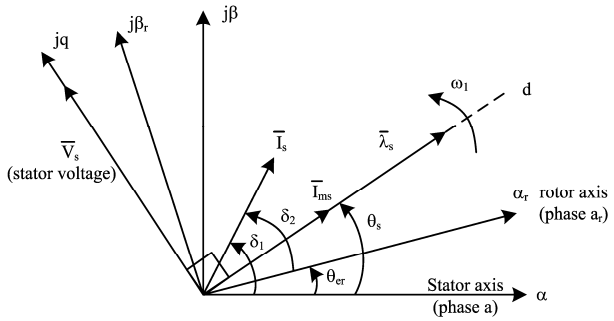

Figure 15.13. Location of rotor current vector $\bar{I}_r$

Let us consider that we know the magnetization curve of the machine, say $I_{ms}(\lambda_s)$ and start with a given value of I_{ms}.

The $\alpha\beta$ components of I_{ms} are evidently (Figure 15.13).

$$\begin{aligned} I_{ms\alpha} &= I_{ms}\cos\theta_s \\ I_{ms\beta} &= I_{ms}\sin\theta_s \end{aligned} \tag{15.32}$$

Then, in stator coordinates, the rotor current components are (from $\bar{I}_r = \bar{I}_{ms} - \bar{I}_s$):

$$\begin{aligned} I_{r\alpha} &= \left(I_{ms\alpha} - I_{s\alpha}\right)\frac{L_s}{L_m};\ \ I_{s\alpha} = I_a \\ I_{r\beta} &= \left(I_{ms\beta} - I_{s\beta}\right)\frac{L_s}{L_m};\ \ I_{s\beta} = \frac{1}{\sqrt{3}}(2I_b + I_a) \\ I_r &= \sqrt{I_{r\alpha}^2 + I_{r\beta}^2} \end{aligned} \tag{15.33}$$

The rotor currents are, however, measured in rotor coordinates, $I_{r\alpha r}$, $I_{r\beta r}$, and:

$$\cos\delta_2 = \frac{I_{r\alpha r}}{I_r},\ \ \sin\delta_2 = \frac{I_{r\beta r}}{I_r}$$
$$I_{r\alpha r} = I_{ar};\ \ I_{r\beta r} = \frac{1}{\sqrt{3}}(2I_{br} + I_{ar}) \tag{15.34}$$

But $\hat{\theta}_{er} = \delta_1 - \delta_2$ and thus:

$$\sin\hat{\theta}_{er} = \sin(\delta_1 - \delta_2) = \sin\delta_1\cos\delta_2 - \cos\delta_1\sin\delta_2 =$$
$$= \frac{I_{r\beta}I_{r\alpha r} - I_{r\alpha}I_{r\beta r}}{I_r^2}$$
$$\cos\hat{\theta}_{er} = \cos(\delta_1 - \delta_2) = \frac{I_{r\alpha}I_{r\alpha r} + I_{r\beta}I_{r\beta r}}{I_r^2} \tag{15.35}$$

Knowing $\cos\hat{\theta}_{er}$ and $\sin\hat{\theta}_{er}$ the rotor speed $\hat{\omega}_r$ is estimated by digital filtering because:

$$\frac{d\hat{\theta}_{er}}{dt} = \hat{\omega}_r = -\sin\theta_{er}\frac{d}{dt}(\cos\theta_{er}) + \cos\theta_{er}\frac{d}{dt}(\sin\theta_{er}) \tag{15.36}$$

To account for magnetic saturation state change (especially during faults when the stator voltage and flux vary notably), after starting the online computation cycle by an initial value of I_{ms}, we will recalculate it as $I'_{ms\alpha}(k)$, $I'_{ms\beta}(k)$, after every computation cycle, in two stages [4]. The magnetization current computation is one step behind but this is acceptable.

$$I'_{ms\alpha}(k) = I_{s\alpha}(k) + \frac{L_m}{L_s}I'_{r\alpha}(k)$$
$$I'_{ms\beta}(k) = I_{s\beta}(k) + \frac{L_m}{L_s}I'_{r\beta}(k) \tag{15.37}$$

With:

$$I'_{r\alpha}(k) = I_{r\alpha r}(k)\cos\hat{\theta}_{er}(k-1) - I_{r\beta r}(k)\sin\hat{\theta}_{er}(k-1)$$
$$I'_{r\beta}(k) = I_{r\beta r}(k)\cos\hat{\theta}_{er}(k-1) + I_{r\alpha r}(k)\sin\hat{\theta}_{er}(k-1) \tag{15.38}$$

15.3.5. The control of the source-side converter

The source-side PWM converter (Figure 15.14) includes at least an LR filter, in order to reduce the source-side current harmonics.

We start with the LR filter equations:

$$\begin{vmatrix} V_a \\ V_b \\ V_c \end{vmatrix} = R \begin{vmatrix} I_{as} \\ I_{bs} \\ I_{cs} \end{vmatrix} + L \frac{d}{dt} \begin{vmatrix} I_{as} \\ I_{bs} \\ I_{cs} \end{vmatrix} + \begin{vmatrix} V_{as} \\ V_{bs} \\ V_{cs} \end{vmatrix} \tag{15.39}$$

After translation into dq synchronous coordinates, aligned with d axis voltage ($V_d=V_s, V_q=0$), equations (15.39) become:

$$\begin{aligned} V_d &= RI_{ds} + L\frac{dI_{ds}}{dt} - \omega_1 LI_{qs} + V_{ds} \\ V_q &= RI_{qs} + L\frac{dI_{qs}}{dt} + \omega_1 LI_{ds} + V_{qs} \end{aligned} \tag{15.40}$$

ω_1 is the frequency of the AC supply voltages.

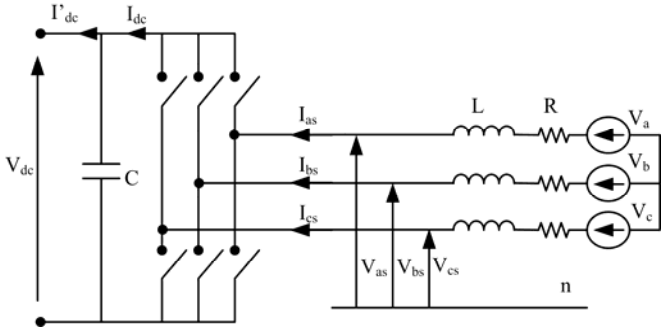

Figure 15.14. The source-side converter with LR filter

Neglecting all losses in the machine and in the converter:

$$V_{dc}I_{dc} = \frac{3}{2}V_d I_d = P_r; V_q = 0 \tag{15.41}$$

With the PWM depth m_1:

$$V_d = \frac{m_1}{2\sqrt{2}}V_{dc} \tag{15.42}$$

Making use of (15.41) in (15.42):

$$I_{dc} = \frac{3m_1 I_d}{4\sqrt{2}} \tag{15.43}$$

The DC link equation writes:

$$C\frac{dV_{dc}}{dt} = I_{dc} - I'_{dc} = \frac{3m_1 I_d}{4\sqrt{2}} - I'_{dc} \tag{15.44}$$

If is thus evident that the DC link voltage may be controlled by controlling the current I_d.

The reactive power Q_r at rotor terminals is:

$$Q_r = \frac{3}{2}\left(V_d I_q - V_q I_d\right) = V_d I_q ; V_q = 0 \tag{15.45}$$

Consequently, the reactive rotor power flow may be controlled by controlling the current I_q. We may add the voltage decoupler:

$$\begin{aligned} V'_{ds} &= V_d + \omega_1 L I_q \\ V'_{qs} &= -\omega_1 L I_q \end{aligned} \tag{15.46}$$

This way a combined voltage/current vector control system ([1], Chapter 9) is born (Figure 15.15)

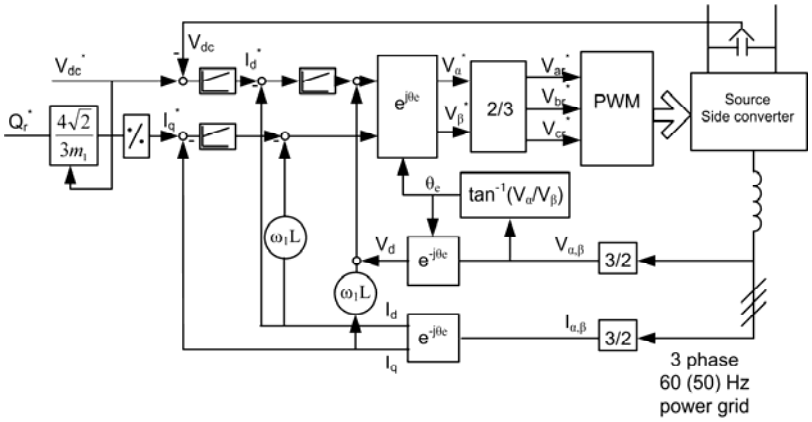

Figure 15.15. Vector control of the source-side converter

For operation at power grid the DC voltage V_{dc} is controlled to remain constant. The Park transformation is operated into two stages (abc to αβ, αβ to dq) and I_d, I_q, V_d, and the voltage vector angle θ_e are calculated from measured I_a, I_b, V_a, V_b. A rather complete design of such a vector control system is given in Ref. 5.

15.3.6. WRIG control – a case study

The case of a wind turbine driving a 2.0 MW WRIG with the following parameters is considered:

V_{SN} (line, RMS) = 690 V, 2p = 4, f_N = 50 Hz, l_m = 3.658P.U., l_{sl} = 0.0634 P.U., l_{rl} = 0.08466 P.U., r_s = 4.694x10^{-3} P.U., r_r = 4.86x10^{-3} P.U., H = 3.611 seconds.

A ±25% maximum slip is considered and, to eliminate the voltage matching transformer from the rotor circuit, the rotor/stator turns ratio $W_r/W_s=1/|S_{max}|$ = 4/1.

The wind turbine is simulated by a 2D – look-up table that produces the mechanical torque T_M as a function of wind speed U (m/s) and generator speed (ω_r) such that to extract maximum power, up to the speed limit.

The control of the source-side converter:

The d-q axis current controllers' design is obtained from the system's transfer function in z-domain with a sampling time T = 0.45 ms. The closed loop natural frequency is 125Hz and the damping factor is 0.8. In these conditions the dc voltage loop PI controller transfer function is 18.69(z-1335.4)/(z-1).

The current controllers' loops are much faster than the DC voltage (V_{dc}) control loop and their transfer function is 17.95 (z-2640) / (z-1).

The generator side converter control:

Again, by imposing the natural close-loop frequency and the damping factor of the plant, the d,q PI current controllers' transfer functions are: 12(z-0.995)/(z-1). The power control loops are much slower with their transfer functions as 0.00009 (z-0.9) / (z-1).

Space vector PWM is used in both converters to generate their reference AC voltages.

Simulation results are obtained through a Matlab/Simulink dedicated program (WRIG.sim – see the attached CD).

At 1.5 seconds in time the wind speed is increased from 7 to 11 m/s, then, at 6 s, the reference value of active power is increased from 0 to 1.2 MW for constant 0.3 MVAR reactive power.

The rotor currents waveforms (Figure 15.16a) and the generator speed (Figure 15.16b) show clearly the smooth passing of the machine through the synchronous speed around 2.1 seconds in time.

The active and reactive power fast transients are shown in Figure 15.16c, d.

A three phase short-circuit at the power grid for same WRIG is illustrated in Figure 15.17. There are two main current peaks, one at the initiation of the short - circuit at half length of a symmetric power line (Figure 15.16e) and the other after the short-circuit.

Decreasing these peaks may be accomplished by simply limiting the output of the current controllers at the machine-side converter at, say 150 % rated value.

This way the WRIG may remain connected to the power grid during the short-circuit, to be ready to contribute to the voltage restoration once the short-circuit is cleared.

15.4. AUTONOMOUS DC EXCITED SYNCHRONOUS GENERATOR

CONTROL AT VARIABLE SPEED

The DC excited synchronous generator may perform as an autonomous power source at constant speed (and voltage) such as in standard standby emergency or gensets, many driven by Diesel engines. In this case, however, the speed (frequency) and voltage are controlled separately such as for power grid operation.

The speed is controlled to remain constant by the speed governor of the prime-mover (Diesel engine) while the voltage is controlled, to stay constant, by the field current control.

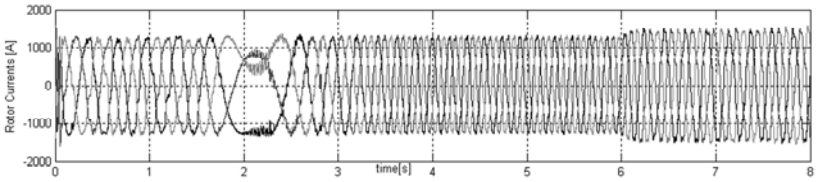

(a)

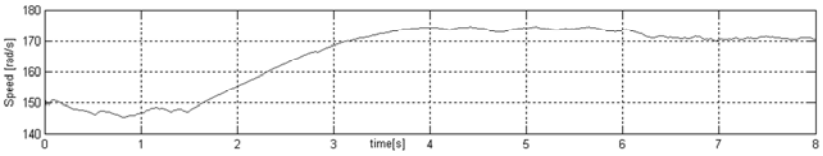

(b)

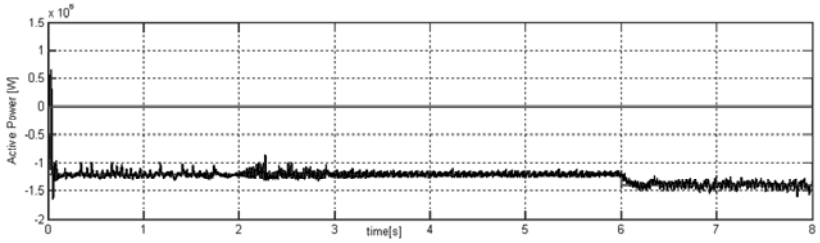

(c)

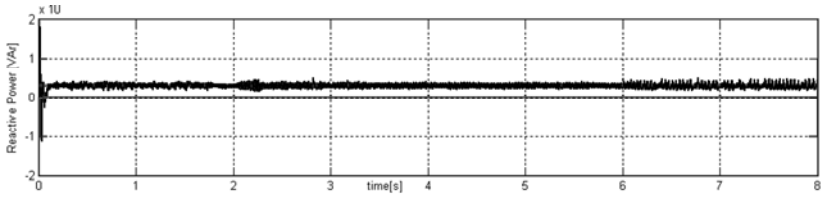

(d)

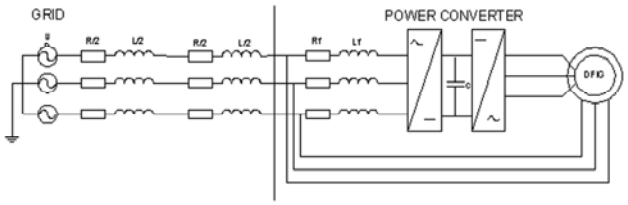

(e)

Figure 15.16. 2MW WRIG transients: a) rotor currents, b) generator speed, c) active power, d) reactive power, e) the system structure

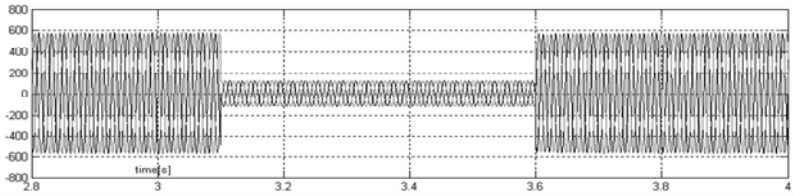

(a)

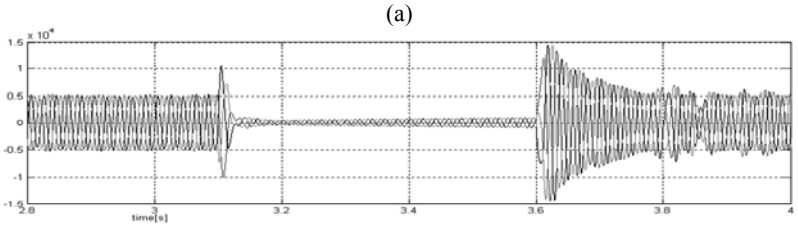

(b)

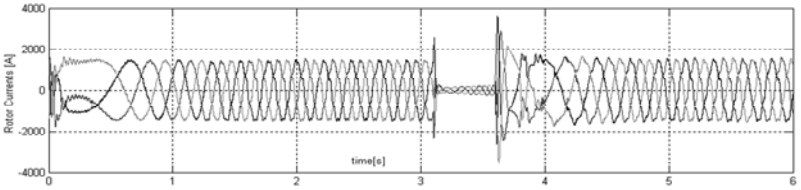

(c)

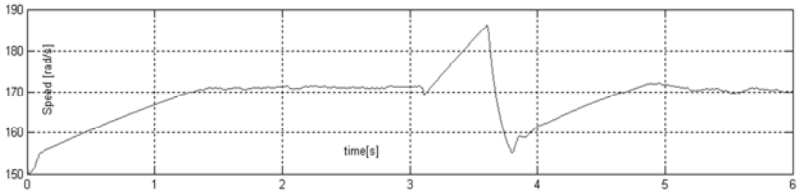

(d)

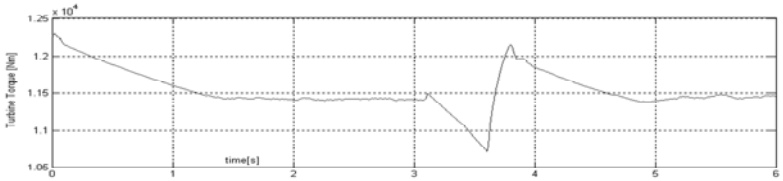

(e)

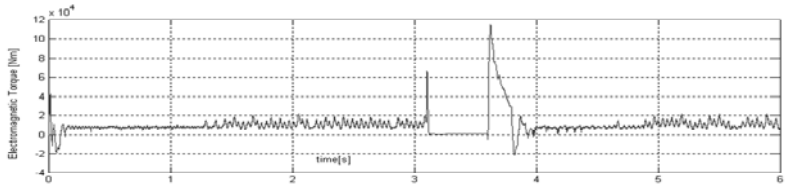

(f)

Figure 15.17. Three phase short-circuit at power grid: a) stator voltage, b) stator currents, c) rotor currents, d) speed, e) turbine torque, f) electromagnetic torque

As this case has been treated in paragraph 15.2, we will dwell here only on variable speed control of DC excited autonomous SG.

Even here there are two main situations:

- With battery back-up and DC controlled output (as for vehicle alternators).
- With AC constant voltage and frequency controlled output.

We will treat both cases in some detail.

15.4.1. Control of the automotive alternator

The automotive industry's alternator is of a single topology: the Lundell - Rice configuration. It has a single ring-shape rotor coil which is DC fed through slip rings and brushes to produce a multipolar (2p = 10, 12, 14, 16, 18) magnetic field in the airgap. The ring-shape rotor coil is surrounded by solid-iron claws to help configure the multipolar magnetic field in the airgap.

The stator is made of standard rotary machine silicon iron laminations with uniform slots that hold a q=1 slot/pole/phase single layer three phase AC winding (Figure 15.18).

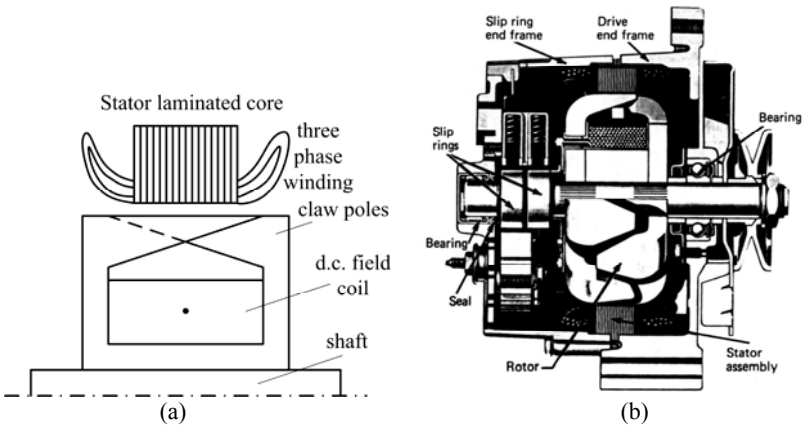

(a) (b)

Figure 15.18. Lundell-Rice automotive alternator: a) cross-section, b) general view

The rotor claw-poles are made of solid iron; so they act as a rather weak damper cage, to be neglected, to a first approximation.

The dq axis reactances X_d and X_q differ from each other ($X_d > X_q$).

The claw-pole alternator is to deliver DC power to the battery – back - up DC loads on automobiles.

To do so, it uses a full power diode rectifier connected between the stator terminals and the battery and a DC field current controller.

The field winding is fed from the alternator terminals through a 3 diode (half) rectifier and a DC - DC converter (Figure 15.19).

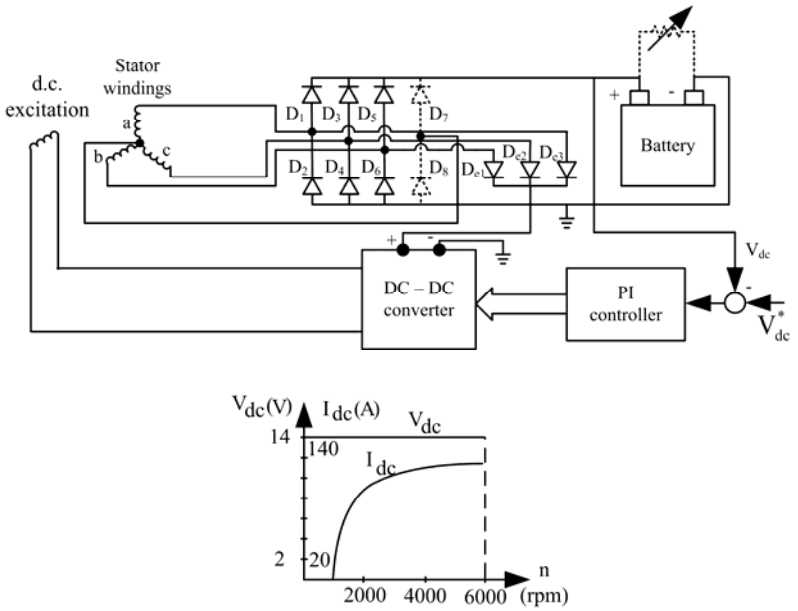

Figure 15.19. Typical automotive alternator control system

Though Figure 15.19 depicts a control system for automotive alternators any variable speed alternator with battery back-up DC output will fit into the category.

A voltage close loop controller is included. For maximum field current the DC output current I_{dc} increases with speed as in Figure 15.19. Slightly below the engine idle speed the DC current is zero because the alternator e.m.f. is insufficient so that the diode rectifier does not open up the energy flow.

The rather large machine transient inductances L'_d, L'_q, due to the weak solid iron rotor claw-poles damping effect, makes the response in DC current, to a step load power increase, not very fast.

As the diode rectifier provides for almost unity power factor, the phasor diagram of the alternator with $L_d \sim L_q$ gets simplified (Figure 15.20).

$$\underline{I}_1 R_s + \underline{V}_1 = \underline{E}_1 - jX_s \underline{I}_1 \tag{15.47}$$

$$\underline{E}_1 = -j\omega_1 X_{dm} \underline{I}_F \tag{15.48}$$

Equations (15.47) – (15.48) have been documented in Chapter 10 but they are straightforward as $\underline{E}_1$ is the e.m.f. and R_s, X_s resistance and cyclic synchronous reactances. $\underline{I}_F$ is the field current equivalent phasor seen from the stator as equations (15.47) are written in stator coordinates.

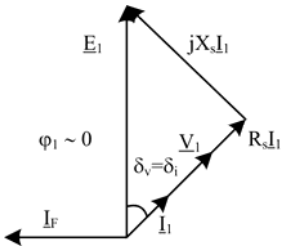

Figure 15.20. The simplified phasor diagram of claw-pole alternator with diode rectifier and $L_d \sim L_q$.

From the power balance:

$$V_1 \approx \frac{V_{dc} I_{dc} + p_{diode}}{3 I_1 \cos\varphi_1}; K_i = \frac{I_{dc}}{I_1} \approx \frac{3\sqrt{3}}{\pi} \cos\varphi_1 \tag{15.49}$$

As the speed increases, E_1 (for a given field current value) and $X_s = \omega_1 L_s$ increase and thus the current I_1 (and I_{dc}) tends to be limited.

From the phasor diagram (with $R_s \sim 0$) the current I_1 is approximately:

$$I_1 = \frac{\sqrt{E_1^2 - V_1^2}}{\omega_1 L_s} \tag{15.50}$$

But, for constant field current I_F:

$$\begin{aligned} E_1 &= K_E(I_F)\omega_1 W_1 \\ X_s &= K_x \omega_1 W_1^2 \end{aligned} \tag{15.51}$$

W_1 is the number of turns/phase and ω_1 is the stator frequency.

Making use of (15.51) in (15.50), the maximum current I_1 is obtained for W_{1opt}:

$$W_{1opt} = \frac{V_1\sqrt{2}}{K_e \omega_1} \text{ or } E_{1opt} = V_1\sqrt{2} \tag{15.52}$$

Consequently, $X_sI_{1opt}=V_1$ for maximum current ($\delta_v = \delta_i = \pi/4$ in Figure 15.20).

It is evident that W_{1opt} should decrease with speed (ω_1) to maintain the maximum optimum current with increasing speed.

Winding tapping or operating at larger voltage are thus practical solutions to increase alternator output current at high speeds. Alternatively, an alternator designed for given power P_n at 14Vdc with a switched mode diode rectifier (as voltage booster) can produce almost twice as much power at high speeds [7] (Figure 15.21) at 42 Vdc.

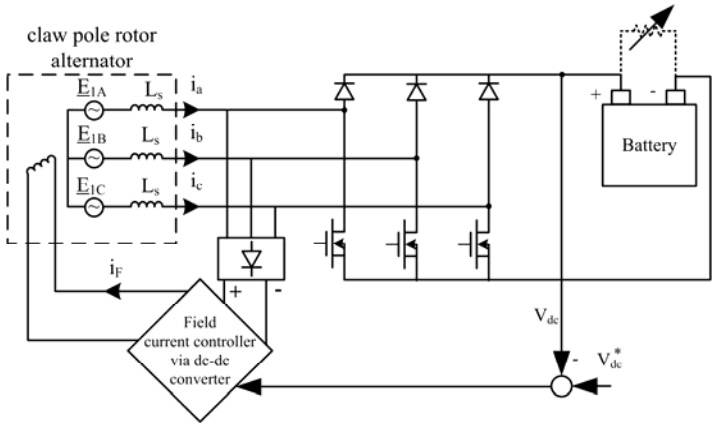

Figure 15.21. Alternator with switched-mode diode rectifier and voltage controller

By operating the automotive alternator at larger DC voltage, not only the output is doubled, but implicitly, the efficiency was improved from less than 50% to 70% [7].

When the load is dumped the maximum voltage has to be limited to 80 Vdc by adequate field current control (protection) provisions, to meet the current standards in automotive industry. Results in Figure 15.22 [7] prove such good performance with the switched-mode rectifier (Figure 15.21).

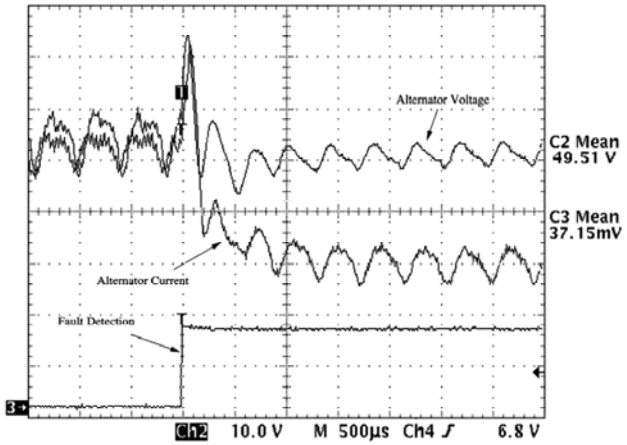

Figure 15.22. Limited load dump voltage transients with the switched-mode diode rectifier

As the electric energy on board the vehicle is on the rise, the adaptation of 42 Vdc bus becomes necessary and beneficial in the sense that today's alternators, designed for 14 Vdc at maximum power P_n, may be used with a switched-mode rectifier and produce $2P_n$ maximum power at 42 Vdc, for increased efficiency.

While efforts to improve the output to efficiency of claw-pole alternators continue, other DC excited alternators such as those with smaller voltage regulation (smaller L_q, with PMs in rotor q axis) have been proposed [8].

15.4.2. AC output autonomous alternator control at variable speed

The autonomous alternator may also provide for constant voltage and frequency output at variable speed (Figure 15.23). A full power PWM inverter is required.

The field circuit is designed and controlled to provide for constant voltage amplitude V_1 (at variable frequency) at alternator terminals for the whole speed range.

Further on, a standard full power diode rectifier with a PWM voltage source inverter will provide for constant frequency and voltage AC output at power grid or for autonomous (separate) loads.

Only unidirectional power flow — from alternator to power grid or to loads — is possible but at moderate costs, as the standard PWM inverter at power grid is similar to an active front end rectifier [9].

V/f standard control of latter is adaptable for autonomous loads when V and f have to be controlled to remain constant with load, up to a point.

It is feasible to use a single DC voltage link for a cluster of alternators and thus a single PWM inverter is required for all of them.

The desired power sharing of each alternator is tailored through its field current controller.

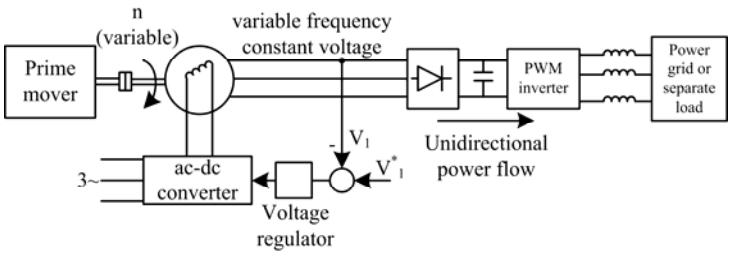

Figure 15.23. Alternator with full power PWM converter control at variable speed

15.5. CAGE-ROTOR INDUCTION GENERATOR CONTROL

The cage-rotor induction machine is known for its ruggedness, moderate costs and rather good performance.

In some applications, such as wind or small hydro energy conversion (up to 1 – 2 MW / unit), variable speed is required to track most of the available wind and hydro energy when the wind speed, and respectively, the water head vary. Also, variable speed with power increasing with generator speed, results in better system efficiency.

One drawback of cage-rotor induction machines is the need for an external source to magnetize them, corroborated with reactive power "production" for voltage control, at constant frequency.

The cage-rotor induction generator (called simply IG) has to be associated with a bidirectional AC-AC power electronic converter in the stator in order to produce active and reactive power control, both at power grid and in stand alone operation. For ±100% P_1 and Q_1 control a back to back PWM voltage source converter (Figure 15.24) is required.

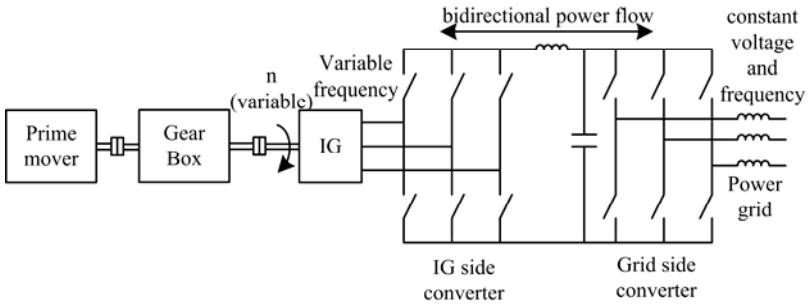

Figure 15.23. IG with back to back PWM converter to power grid:

±100% P_1 and Q_1 control

The bidirectional back to back PWM inverter contains the grid-side converter and the IG side converter. The source-side converter control is the same as for WRIG (see paragraph 13.3) where this converter was connected to the rotor. In essence, for power grid operation, the vector control in grid voltage coordinates is used such that the active power flow is controlled by controlling the DC link voltage along axis d and the reactive power Q_1 along axis q. But in this case the DC link capacitor has to be designed for ±100% reactive power control. This way the IG behaves towards the loads as a synchronous generator, with faster ±100 % active and reactive power control.

The IG side converter may be either vector or direct torque and flux control type (DTFC), for motoring and generating, as widely discussed in Chapter 9 on induction motor drives.

When the IG works in autonomous load mode, the load side converter may be either vector or V/f controlled, for constant or drooped voltage amplitude control and constant frequency output control (for more details see Reference 1, Chapter 13). Typical AC grid side voltage and current waveforms for 100% active power and zero reactive power control of an 11KW IG (connected to an off the shelf bidirectional back to back PWM converter designed for fast braking electric drives) is shown in Figure 15.25 ([1], Chapter 13).

More filtering of the current is required to meet the today's strict harmonics content limitation standards.

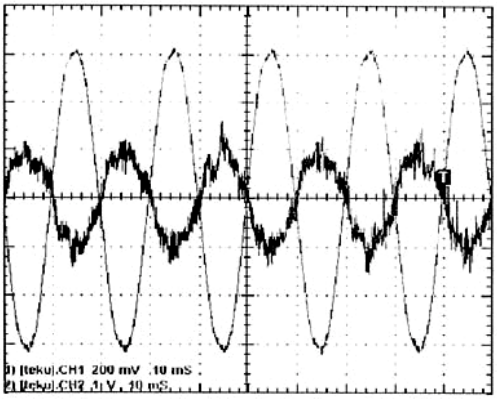

Figure 15.25. Grid voltage and current at 1500 rpm for generator mode at 100 % active and zero reactive power control

15.6. PM SYNCHRONOUS GENERATOR CONTROL FOR VARIABLE SPEED

PM synchronous generators (PMSG) are built either with surface-pole PM or interior PM rotor, with radial or axial airgap, with distributed or non - overlapping windings, just as PM synchronous motors (Chapter 10).

For convenience we will show here only the radial-airgap, distributed stator winding configuration with surface-pole-PM and, respectively, inset-pole-PM rotor (Figure 15.26).

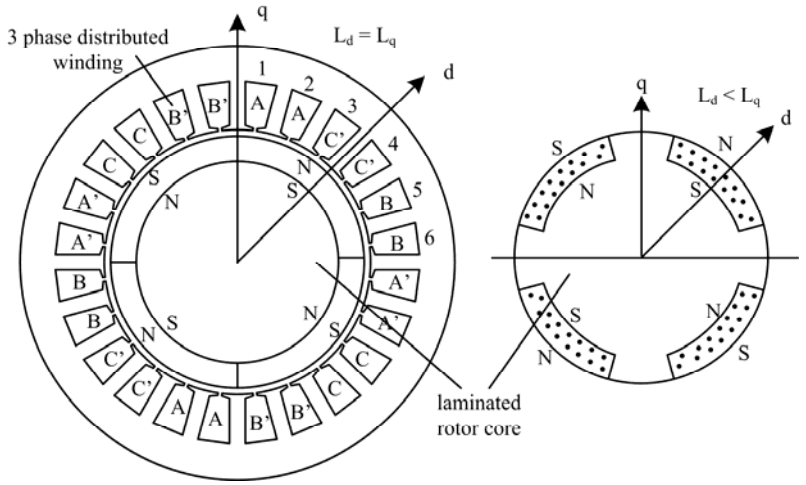

Figure 15.26. PMSG with distributed single layer stator winding ($2p_1$=4, N_c=24 slots): a) surface PM-pole rotor, b) inset-PM-pole rotor

In essence, the distributed three phase winding in Figure 15.26 is characterized by rather sinusoidal stator phase e.m.f.s. However, as a single layer winding is chosen, the stator current m.m.f. produces notable 5 and 7 space harmonics which, in turn, may produce notable eddy current losses in the rotor PMs.

Surface PM pole rotors are characterized by the zero magnetic saliency (L_d=L_q) while inset-PMs may lead to a special design when, for rated resistive load, the rated PMSG voltage V_{1N} is equal to no load voltage E_1, for given speed (Figure 15.27).

The phasor diagram for the two rotors (Figure 15.27) is based on the phase equations:

$$\underline{I}_1 R_s + \underline{V}_1 = \underline{E}_1 - jX_d \underline{I}_d - jX_q \underline{I}_q ; \underline{I}_1 = \underline{I}_d + \underline{I}_q$$
$$\underline{E}_1 = -j\omega_1 \lambda_{PM} \qquad (15.53)$$

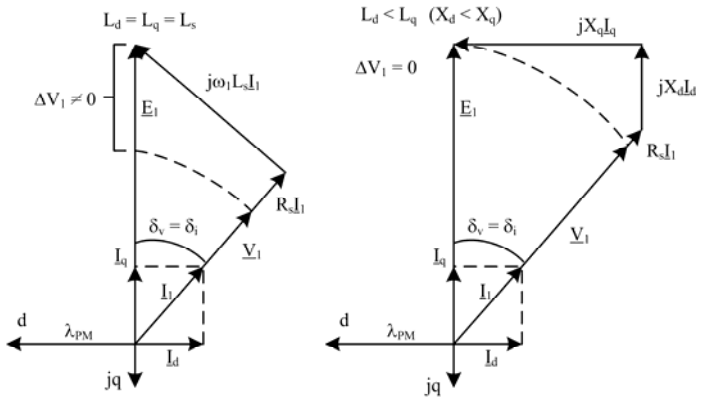

Figure 15.27. The phasor diagram of PMSG on resistive (or diode rectifier) load: a) with surface–PM–pole rotor, b) with inset-PM-pole rotor

The dq model of the PMSG is practically the same as for PMSM (Chapter 10):

$$\begin{aligned} I_d R_s + V_d &= -L_d \frac{dI_d}{dt} + \omega_r \lambda_q;\ \ \lambda_d = L_d I_d + \lambda_{PM} \\ I_q R_s + V_q &= -L_q \frac{dI_q}{dt} - \omega_r \lambda_d;\ \ \lambda_q = L_q I_q \end{aligned} \tag{15.54}$$

$$\begin{aligned} V_d &= \frac{2}{3}\left(V_a \cos(-\theta_{er}) + V_b \cos(-\theta_{er} + \frac{2\pi}{3}) + V_c \cos(-\theta_{er} - \frac{2\pi}{3}) \right) \\ V_q &= \frac{2}{3}\left(V_a \sin(-\theta_{er}) + V_b \sin(-\theta_{er} + \frac{2\pi}{3}) + V_c \sin(-\theta_{er} - \frac{2\pi}{3}) \right) \end{aligned} \tag{15.55}$$

The electromagnetic torque writes (Chapter 10):

$$T_e = \frac{3}{2} p(\lambda_d I_q - \lambda_q I_d) = \frac{3}{2} p\left(\lambda_{PM} + (L_d - L_q) I_d\right) \cdot I_q \tag{15.56}$$

As the equations are written for generator association of signs $T_e>0$ for generator. Negative torque (motoring) is obtained with negative I_q.

The motion equations have to be added:

$$\frac{J}{p}\frac{d\omega_r}{dt} = T_{mec} - T_e;\ \frac{d\theta_{er}}{dt} = \omega_r \tag{15.57}$$

The prime mover torque $T_{mec}>0$ for PMSG generator operation mode and negative for PMSG motoring operation.

Let us take a numerical example to calculate PMSG steady state performance.

Example 15.1.

Let us consider a surface-PM-pole rotor PMSG with the data: R_s=0.1Ω, L_s=L_d=L_q=0.005H, λ_{PM}=0.5Wb, p_1=2 pole pairs, that has to deliver power into a three phase resistance R_L=3Ω/phase at n_1=1800rpm:

a) Calculate the phase current, voltage and power.

b) For same phase current, calculate the load resistance R'_L and power and L_q>L_d (inset-PM-pole rotor), when the load voltage V_{1r}=E_1 (e.m.f.).

Solution:

a) The equations (15.54) apply directly for V_d=$R_L I_d$, V_q=$R_L I_q$ and d/dt=0:

$$(R_s + R_L)I_d = \omega_r L_q I_q$$
$$(R_s + R_L)I_q = -\omega_r(\lambda_{PM} + L_d I_d)$$

Or:

$$(0.1+3)I_d = 2\pi \cdot 30 \cdot 2 \cdot 0.005 \cdot I_q \qquad I_d = -19.5766\text{A}$$
$$(0.1+3)I_q = -2\pi \cdot 30 \cdot 2(0.5 + 0.005 \cdot I_d) \rightarrow I_q = -53.664\text{A}$$

The phase current I_1 is:

$$I_1 = \sqrt{\frac{1}{2}\left(I_d^2 + I_q^2\right)} = 40.3922\text{A(rms)}$$

Consequently, the delivered power P_1 writes:

$$P_1 = 3R_L I_1^2 = 14.683\text{KW}$$

The phase voltage V_1 is:

$$V_1 = R_L I_1 = 121.1766\text{V(rms/phase)}$$

b) For zero voltage regulation:

$$V_{1r} = E_1 = 2\pi \cdot 30 \cdot 2 \cdot 0.5 = 188.5\text{V(rms/phase)}$$

If the current I_1 is kept the same, the power is delivered on a new load resistance R'_L:

$$R'_L = \frac{V_{1r}}{I_1} = 4.6667\ \Omega/\text{phase}$$

We return to the above equations with known R_s, R'_L, L_d and I_1, and need to find out L_q (or I_d):

$$(0.1 + 4.6667)I_q = -377(0.5 + 0.005I_d)$$
$$4.7667I_d = 377L_q I_q$$

From the first equation with $I_q = \sqrt{3264 - I_d^2}$, we finally calculate:

$$I_d = -31.128A$$

Consequently:

$$L_q = \frac{4.7667 \cdot (-31.128)}{377 \cdot (-47.906)} = 0.00821H$$

$L_q/L_d=0.00821/0.005=1.643$, a ratio which may be reached with inset-PMs on the rotor if only with a slightly smaller mechanical airgap.

The power delivered now is:

$$P_1^{'} = 3R_L^{'} I_1^2 = 23.153W$$

Consequently, 57.69 % more power is gained from basically same machine and stator windings losses, just by using inset magnets on the rotor poles. Definitely the inverse saliency seems to pay off.

15.6.1. Control schemes for PMSG

The PMSG may work alone or at power grid. Let us consider the power grid operation, at variable speed, by two essential power electronics control configurations (Figure 15.28).

The voltage booster active switch T_1 (Figure 15.28a) makes use of machine inductances and the additional L_{dc} to boost the voltage in the DC link in a controllable manner.

A constant DC voltage link may be secured from ω_{rmin} to ω_{rmax}, provided there is still room at ω_{rmax} to boost a little the DC link voltage, to keep T_1 active.

The grid side PWM inverter is controlled as for the WRIG (paragraph 15.3).

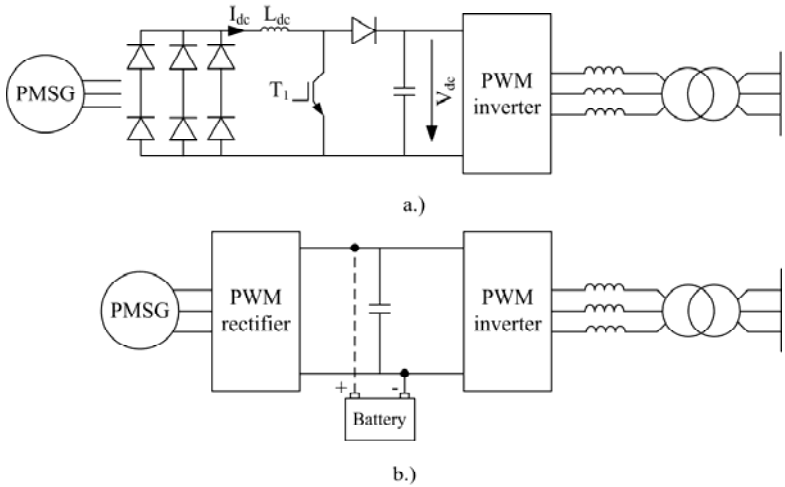

Figure 15.28. Variable speed PMSG with constant voltage and frequency AC output:
a) with hard - switched diode – rectifier and PWM inverter;
b) with active front rectifier and PWM inverter

On the other hand, if motoring (for starting the prime mover) is required, an active front end rectifier is required on the machine side (Figure 15.28b). This PWM converter is to be controlled as for motoring and regenerative braking of PMSM. Vector or direct torque (or power) and flux control (DTFC), as in Chapter 11 for PMSM drives, is applicable with or without motion sensors.

On the other hand, the PMSG may work as a stand alone generator driven by a medium speed Diesel engine or by a high speed gas turbine. Standby emergency or remote-area electric energy generation require such solutions. Again, the load side PWM converter may be V/f or vector controlled with an output harmonics power filter as for the IG.

An up to date Diesel engine PMSG system with multiple output frequency, single phase and three phase AC output, for variable speed, with fuel saving, is presented in Reference 10.

15.7. SWITCHED RELUCTANCE GENERATOR (SRG) CONTROL

The switched reluctance machine (SRM), which can be built in single phase or multiphase configurations, may work as a motor or as a generator.

Motoring is required if the prime-mover starting or assistance is required as in hybrid electric vehicles [1, 11-12].

If only generator operation is necessary, single phase (for low power) and three phase configurations seem favorite.

The circuit mathematical model of SRM developed in Chapter 12 holds valid here and thus will not be derived again.

We will rather concentrate on typical current waveforms for generator mode, typical PWM converters and a voltage controller for DC output at variable speed.

The SRG current waveforms

The turn on θ_{on} and θ_{off} angles for generator mode occur at the beginning, and respectively long before the end of negative inductance slope of the conducting phase (Figure 15.28a).

The phase i voltage equation is:

$$V_i = R_s I_i + L_{ti}(I_i, \theta_r)\frac{dI_i}{dt} + K_E(I_i, \theta_r)\cdot 2\pi n \tag{15.58}$$

K_E is the pseudo e.m.f. coefficient.

$$E = K_E 2\pi n;\ \ K_E(I_i, \theta_r) = I_i \frac{\partial L_i}{\partial \theta_r} < 0, \text{for generating} \tag{15.59}$$

We may consider $L_{ti} \cong L_u$ (unaligned) = constant for the heavily saturated core machine.

Voltage $V_i = +V_{dc}$ for phase energization and $V_i = -V_{dc}$ during power delivery (phase de-energization).

There are three generator operation modes as illustrated in Figure 15.29a, b.

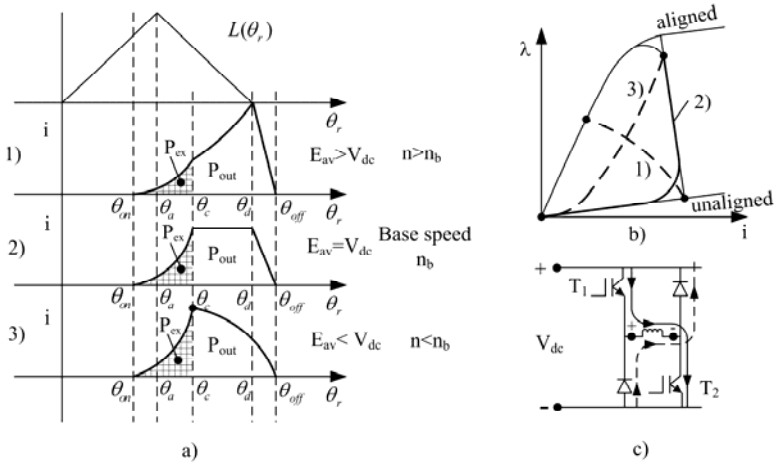

Figure 15.29. SRG: a) inductance/position and current waveforms, b) corresponding energy cycles, c) typical phase PWM converter.

As during generator mode $V_i = -V_{dc} < 0$ and $E < 0$, the current which remains positive increases as long as $|E|>|V_{dc}|$. This case is typical for high speeds when the torque (energy cycle area) is smaller (Figure 15.29b, cycle 1).

For case a2 in Figure 15.29a, at the turn off angle θ_c, $|\underline{E}| = V_{dc}$ and thus, with $R_s \sim 0, di/dt = 0$, the current stays constant until the phase inductance reaches its minimum at angle θ_d (Energy cycle 2 in Figure 15.28b).

In case a3 in Figure 15.29a the maximum current is reached at θ_c and, after that, the current decreases monotonously because $|E| < V_{dc}$, which corresponds to low speeds (energy cycle 3 in Figure 15.29b).

For constant DC voltage power delivery, the excitation (energization) energy per cycle W_{exc} is:

$$W_{exc} \approx \frac{V_{dc}}{2\pi n} \int_{\theta on}^{\theta c} i d\theta_r \tag{15.60}$$

while the energy delivered per cycle W_{out} is:

$$W_{out} \approx \frac{V_{dc}}{2\pi n} \int_{\theta c}^{\theta off} i d\theta_r \tag{15.61}$$

We may define the excitation penalty ε as:

$$\varepsilon = \frac{W_{exc}}{W_{out}} \tag{15.62}$$

$|E| > V_{dc}$ leads to a smaller excitation penalty but not necessarily to the highest energy conversion ratio, which seems to correspond to $|E| \sim V_{dc}$.

Maintaining this latter condition, however, it means to increase V_{dc} with speed because E increases with speed. A step down DC-DC converter has to be added as the DC output voltage has to stay constant for ω_{rmin} to ω_{rmax}.

To control the power output, the turn on and turn off angles θ_{on} and θ_c should be changed in a certain manner.

If such a step-down DC converter is not available, then the generator mode will evolve from case a1 ($|E| < V_{dc}$), below base speed, to case a2 ($|E| = V_{dc}$) and a3 ($|E| > V_{dc}$) — Figure 15.29 — as the speed increases. A rather moderate speed range constant output voltage control is provided this way.

An average excitation penalty ε = 0.3-0.4 should be considered acceptable for good energy conversion ratio, though a notable energy reserve is lost.

Typical static power converters for $|E| = V_{dc}$ and, respectively, variable $|E|/V_{dc}$ ratio (with speed) control are shown in Figure 15.30.

The additional boost capability, to the buck converter is required when motoring is needed, as for starter-alternators on hybrid vehicles (Figure 15.30a).

To stabilize the output voltage of stand-alone loads it may be suitable to supply the excitation power from a separate battery (Figure 15.30b, left). The diode D_{oe} allows for battery assistance during generating mode and thus the battery cost is rather small.

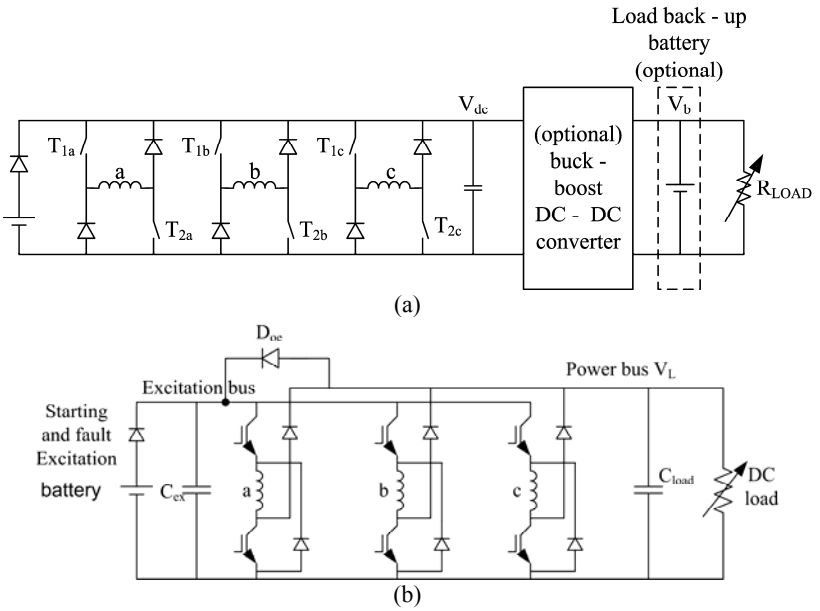

Figure 15.30. Three SRG: a) with asymmetrical PWM converter, self excitation (from battery) or load back-up battery and DC-DC converter; b) with separate excitation power bus and fault clearing capability

The excitation battery also allows SRG to operate during load faults and clear them quickly (Figure 15.31) [15].

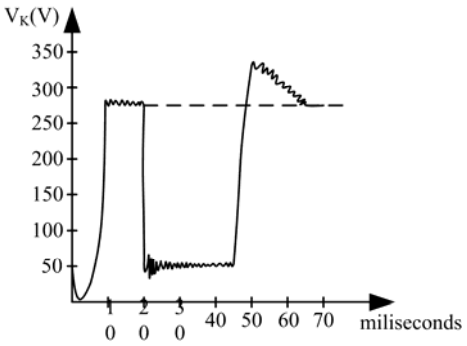

Figure 15.31. SRG voltage rise-up, experiencing a fault (by sharp load resistance reduction) and voltage swift recovery

Intricate SRG control at variable speed for electric vehicles is demonstrated in Reference [14] with feedforward torque control and in Reference [15-17] with direct torque control.

The ruggedness of SRG and its wide speed range constant power capability at constant DC voltage are strong assets in its favor, especially in battery back-up DC loads, typical for automobiles, ships and aircraft.

15.8. SUMMARY

- Practically all electric energy is produced (from primary fuel energy) through electric generators driven by prime-movers (turbines).
- In today's standard electric power systems many synchronous electric generators are connected in parallel.
- Their voltage (reactive power) and speed (active power) is controlled with a small droop to allow for desired power sharing between paralleled synchronous generators.
- The voltage (reactive power) control of SG is performed through the SG excitation current; an exciter source is required; it may be a brushless AC exciter or a static exciter. Fast voltage recovery response is required; various automatic voltage regulators have been proposed and a PID digital version is illustrated in this chapter.
- While SGs in power systems are controlled with a small speed droop, when they act alone on a few loads their speed is controlled either to stay constant or is left to vary (to reduce speed with power decrease) to save fuel in the prime-mover, when a full power converter is needed to yield constant voltage and frequency output over the entire speed range.
- SGs are present on automobiles as alternators with full power diode rectifier output to a DC battery. The alternator provides DC current in the battery, increasing with speed through proper DC excitation current control via voltage close loop regulator and a low power electronics converter.
- For wind and small hydro energy conversion in the MW/unit range variable speed for best primary energy tapping and better stability, the doubly-fed (wound rotor) induction generator (WRIG) is used.
- WRIG contains a dual (AC-DC-AC) PWM converter connected to the wound rotor through brushes and slip-rings. This converter is feeding the rotor with a voltage $V_r \leq V_s$ at a frequency $f_2 = f_1 - np >< 0$; (V_r ,V_s, rotor and stator voltages, f_2, f_1 – rotor and stator frequency, n – speed rps, and p – pole pairs). The speed range is defined by the maximum slip $S_{max} = \pm(5\text{-}30)\ \% = f_2/f_1$; smaller values are typical for larger powers.
- The PWM bidirectional converter is practically rated at $|S_{max}|P_n < 30\%P_n$ and thus lower system costs are obtained.
- WRIG has been implemented up to 400 MW/unit in pump storage hydro - generators. The fast active and reactive power control within the speed range from 70 % to 130 % of rated speed is a flexibility asset that fixed speed SGs are lacking. WRIG is practically an SG at all speeds within the speed range and its synchronization to the grid is very quick and safe.

- Cage rotor induction generators with full power bidirectional PWM converters connected to the stators seem the favorite solution in wind, small hydro and even gensets up to 1-2 MW/unit as they provide fast smooth connection to the power grid. From the grid point of view they behave like very fast controlled SGs, but at variable speed.
- Permanent magnet synchronous generators are characterized by low losses and, for inset (or interior) PM – rotor, they may exhibit even zero voltage regulation on resistive rated load.
- PMSG may be controlled for variable speed with constant DC voltage output or with constant frequency and voltage output, when a full power electronic converter is required. PMSG may work in stand alone applications (starter/alternators on cars) or in power grid applications, driven by high speed gas turbines to produce cogeneration or emergency, or peak power in various applications.
- Switched reluctance generators have been proposed especially for vehicle applications (automobile and aircraft starter alternators) at variable speed, when they deliver power on DC battery back-up loads.
- Electric generator control is needed both in power systems, now still standard but more distributed in the future, and also in stand alone vehicular or on ground applications. Decentralized, controlled, electric energy production requires variable speed in general and thus power electronics control of active and reactive power comes into play.
- As for electric motor operation mode, there is a myriad of electric generators with their digital control via power electronics for better energy conversion and higher power quality.
- Control of electric generators at variable speed can collect from the immense heritage of electric drives control techniques, and should constitute a major technology of the future.
- The present chapter should be considered only a tiny introduction to EG control; see Reference 1 to start your own journey into this field.

15.9. SELECTED REFERENCES

1. **I. Boldea,** Electric generators Handbook, Part 1/2 and 2/2, Taylor and Francis, 2005.
2. **P. Kundur,** Power systems stability and control, MacGraw Hill, 1994.
3. **A. Godhwani, M.J. Bassler,** "A digital excitation control system for use on brushless excited synchronous generators", IEEE – Trans, Vol. EC – 11, no. 3, 1996, pp. 616-620.
4. **R. Datta, V.T. Ranganathan,** "A simple position – sensorless algorithm for rotor-side field oriented control of wound rotor induction machine", IEEE-Trans. Vol. IE – 48, no. 4, 2001, pp. 786-793.
5. **R. Rena, J.C. Clare, G.M. Asher,** "Doubly fed induction generator using back to back PWM converters and its application to variable speed wind-energy generation", Proc. IEE, Vol. EPA – 143, no. 3, 1996, pp. 231-241.
6. **I. Serban, F. Blaabjerg, I. Boldea, Z. Chen,** "A study of the double fed wind power generator under power system faults", Record of EPE-2003, Toulouse, France.
7. **D.J. Perreault, V. Caliskan,** "Automotive power generation and control", IEEE Trans.

Vol. PE – 19, no. 3, 2004, pp. 618-630.

8. **S. Scridon, I. Boldea, L. Tutelea, F. Blaabjerg, E. Ritchie,** "BEGA – a biaxial excitation generator for automobiles: comprehensive characterization and test results", Record of IEEE-IAS-2004, Seattle, USA.
9. **M. Kazmierkowski, R. Krishnan, F. Blaabjerg (editors),** Control in power electronics, Academic Press, Amsterdam, 2002.
10. **L.M. Tolbert, W.A. Peterson, T.J. Theiss, M.B. Sardiere,** "Gen-sets", IEEE-IA Magazine, vol. 9, no. 2, 2003, pp. 48-54.
11. **J. Hussain,** Electric and hybrid vehicles, CRC Press, Florida, 2003.
12. **A. Emadi, M. Ehsani, J.M. Miller,** Vehicular electric power systems, Marcel Dekker, New York, 2004.
13. **A.V. Radun, C.A. Ferreira, E. Richter,** "Two channel switched reluctance starter-generator results", IEEE Trans. Vol. IA-34, no. 5, 1998, pp. 1106-1109.
14. **H. Bausch, A. Grief, K. Kanelis, A. Mickel,** "Torque control battery supplied switched reluctance drives for electrical vehicles", Record of ICEM – 1998, vol. 1, pp. 229-234.
15. **R.B. Inderka, R.W. De Doncker,** "Simple average torque estimation for control of switched reluctance machines", Record of EPE-PEMC-2000, Kosice, Vol. 5, pp. 176-181.
16. **S. Dixon, B. Fahimi,** "Enhancement of output electric power in SRGs", Record of IEEE-IEMDC-2003, Madison, Wi, Vol. 2, pp. 849-856.